msp

Geometry & Topology 19 (2015) 1657–1683

"Slicing" the Hopf link

VYACHESLAV KRUSHKAL

A link in the 3–sphere is called (smoothly) slice if its components bound disjoint smoothly embedded disks in the 4–ball. More generally, given a 4–manifold M with a distinguished circle in its boundary, a link in the 3–sphere is called *M–slice* if its components bound in the 4–ball disjoint embedded copies of M. A 4–manifold M is constructed such that the Borromean rings are not M–slice but the Hopf link is. This contrasts the classical link-slice setting where the Hopf link may be thought of as "the most nonslice" link. Further examples and an obstruction for a family of decompositions of the 4–ball are discussed in the context of the A-B slice problem.

57N13; 57M25, 57M27

1 Introduction

The classification of knots and links up to concordance, and in particular the study of slice links, is a classical and challenging problem at the interface between 3– and 4–manifold topology. Recall that a link in the 3–sphere is called smoothly (respectively topologically) *slice* if its components bound disjoint smooth (respectively locally flat) embedded disks in the 4–ball, where $S^3 = \partial D^4$. The results of this paper take place in the smooth category, so without further mention all 4–manifolds and maps between them will be smooth.

Let M be a 4–manifold with a distinguished circle in its boundary $\gamma \subset \partial M$, embedded in the 4–ball: $(M, \gamma) \subset (D^4, S^3)$. A link $L = (l_1, \dots, l_n)$ in the 3–sphere is called *M–slice* if there exist n disjoint embeddings $f_i\colon (M, \gamma) \hookrightarrow (D^4, S^3)$ such that $f_i(\gamma) = l_i$, $i = 1, \dots, n$. The classical notion of a slice link corresponds to M equal to the 2–handle: $(M, \gamma) = (D^2 \times D^2, \partial D^2 \times 0)$. The more general notion of M–slice links is considerably more subtle, with the topology of M playing an important role. In particular, a new feature not present in the classical setting is that 1– and 2–handles of M may link when M is embedded in D^4. We impose an additional requirement in the definition of M–slice that each embedding f_i is isotopic to the original embedding $(M, \gamma) \subset (D^4, S^3)$. This condition, motivated by the A-B slice problem (see Section 5.1), gives some control over the complexity of the problem, for example allowing one to keep track of the linking of the handles of M in 4–space. (It

Published: 21 May 2015 DOI: 10.2140/gt.2015.19.1657

follows from the Krushkal [6] that the resulting theory is quite different depending on whether this requirement is imposed or not. This is discussed in more detail further below.) The main result of this paper is the following theorem.

Theorem 1 *There exist 4–manifolds M such that the Hopf link is M–slice but the Borromean rings are not.*

This result contrasts the usual slice setting: Note that any link in S^3 bounds smooth disks in D^4, possibly intersecting and self-intersecting in a finite number of transverse double points. The intersections (and self-intersections) of surfaces in 4–space are locally modeled on two coordinate planes intersecting at the origin in $\mathbb{R}^4$, and the link of the singularity is the Hopf link. Thus in a naive sense, "if the Hopf link were slice the double points could be resolved and any link would be slice". In this imprecise sense, the Hopf link plays a role in link theory analogous to that of the free group F on two generators in group theory: The Hopf link is "the most nonslice link" similarly to F being "the most nonabelian group". The theorem above shows that this analogy does not extend to the more general notion of M–slice links.

The manifold M in the proof of the theorem is constructed in Section 2 as a handlebody with 1– and 2–handles, and the embedding/nonembedding results are proved in the *relative-slice* context introduced by Freedman and Lin in [3]. Here the 1–handles embedded in D^4 are dually considered as 2–handles removed from the collar on the boundary, and the embedding question is equivalent to slicing the attaching link for the 2–handles "relative to" the link corresponding to the 1–handles. The fact that the Hopf link is M–slice is proved in Section 3, using properties of the Milnor group [9] adapted to the relative-slice context. The second part of the theorem, asserting that the Borromean rings are not M–slice, relies on a subtle calculation in commutator calculus; see Section 4.

The notion of an M–slice link arises naturally in the *A-B slice problem* (see Freedman [1] and [3]), a formulation of the 4–dimensional topological surgery conjecture. The analysis necessary for finding an obstruction for the Borromean rings in Theorem 1 is quite different compared to previously considered examples in the subject. In particular, this is the first observed case where the system of equations associated to the relative-slice problem has *rational* but not integral solutions. If the answer to the A-B slice problem turns out to be positive (ie if surgery works for free groups), then it seems likely that the phenomena observed in this paper will have a role in constructing the relevant A-B decompositions. On the other hand, the results of the paper are consistent with the conjecture [1] that the Borromean rings are not A-B slice; see Section 5 for further discussion.

2 Construction of M

The starting point of the construction is the handlebody $A_0 = S^1 \times D^2 \times [0,1] \cup$(two zero-framed 2–handles), where the 2–handles are attached to the Bing double of the core of the solid torus $S^1 \times D^2 \times \{1\}$; see Figure 1.

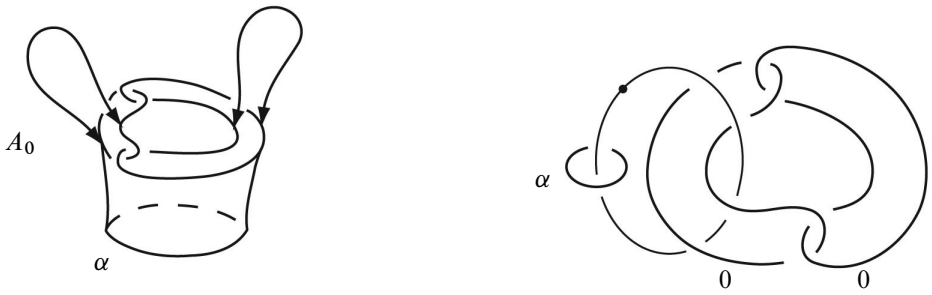

Figure 1: A preliminary construction: zero-framed 2–handles attached to the Bing double, a schematic picture of the spine and a Kirby diagram

The distinguished circle ("attaching curve") of A_0 is $\alpha = S^1 \times \{0\} \times \{0\}$. This handlebody is easily seen to embed into D^4; it is the complement of a standard embedding into D^4 of a genus-one surface with boundary: $D^4 = A_0 \cup B_0$, where $B_0 = \Sigma \times D^2$, Σ is a genus surface with $\partial\Sigma = \beta$, and the curves α, β form the Hopf link in ∂D^4. Iterating this construction (applying the Bing doubling described above) to various 2–handles of A_0, B_0 one gets the family of *model decompositions* of the 4–ball; see [3] and also Freedman and the author [2] for more details. The construction in this paper builds on recent work of the author in [6; 7], and it is quite different from the model decompositions.

The relevant 4–manifold A used in the proof of Theorem 1 is obtained by attaching a single 1–handle to A_0, as shown on the left in Figure 2. (The actual manifold M in the statement of Theorem 1 will be defined as A with a number of self-plumbings of its 2–handles; see Section 3.4.) To avoid drawing unnecessarily complicated diagrams later in the paper, a short-hand handle notation for A is introduced on the right in Figure 2.

Note that the link formed by the two dotted components is the two-component unlink, and the diagram in Figure 2 is indeed a Kirby diagram of a 4–manifold. There is a band visible in the picture which is involved in the connected sum of "parallel copies" of the two zero-framed 2–handles (they are not actual parallel copies since the dotted curve on the left and the attaching curves of the two 2–handles form the Borromean rings, while the dotted curve on the left and the two "parallel copies" form the unlink

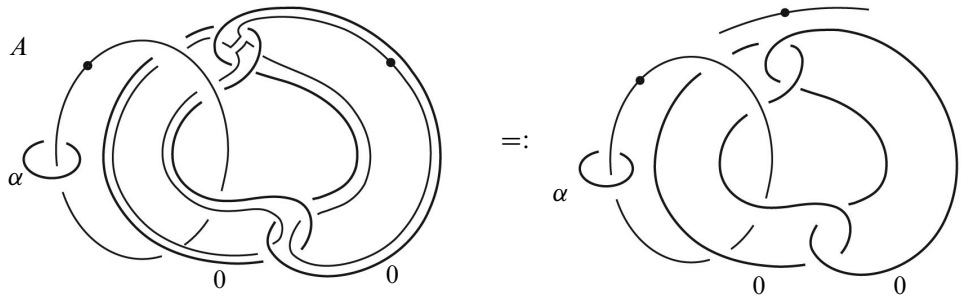

Figure 2: A Kirby diagram of the 4–manifold A: The figure on the right will serve as a shorthand notation for A in follow-up sections to avoid drawing the complicated dotted curve.

as shown on the right in Figure 12). A particular choice of this band in the 3–sphere is not going to be important for the argument, as long as the dotted link is the unlink. The construction in Figure 2 differs from an example in [6; 7] in the attaching curve of the "interesting" 1–handle. The properties of the resulting 4–manifolds are quite different, and the analysis required to formulate an obstruction for the Borromean rings in this paper is substantially more subtle. This work sheds a new light on the techniques necessary for a solution to the A-B slice problem; see Section 5.

3 The Hopf link is M–slice

The proof of Theorem 1 will be given in the following two sections in the context of the *relative-slice* problem (introduced in [3] and also described below) using the Milnor group. The reader is referred to the original reference [9] for a more complete introduction to the Milnor group of links in the 3–sphere. The application in this paper will concern a variation of the theory for submanifolds in 4–space which will be summarized next.

3.1 The Milnor group

Definition 3.1 Let G be a group normally generated by a finite collection of elements $g_1, \dots, g_n$. The *Milnor group* of G, relative to the given normal generating set $\{g_i\}$, is defined as

$$MG := G/\langle\langle [g_i^x, g_i^y] \mid i = 1, \dots, n,\ x, y \in G \rangle\rangle. \tag{3-1}$$

The Milnor group is a finitely presented nilpotent group of class less than or equal to n, where n is the number of normal generators in the definition above; see [9].

Suppose Σ is a collection of surfaces with boundary, properly and disjointly embedded in (D^4, S^3), and let G denote $\pi_1(D^4 \smallsetminus \Sigma)$.

Consider meridians m_i to the components Σ_i of Σ: m_i is an element of G which is obtained by following a path α_i in $D^4 \smallsetminus \Sigma$ from the basepoint to the boundary of a regular neighborhood of Σ_i, followed by a small circle (a fiber of the circle normal bundle) linking Σ_i, then followed by α_i^{-1}. Observe that G is normally generated by the elements $\{m_i\}$, one for each component of Σ.

Let $F_{g_1,\dots,g_n}$ denote the free group generated by the $\{g_i\}$, $i = 1, \dots, n$, and consider the Magnus expansion

$$M\colon F_{g_1,\dots,g_n} \longrightarrow \mathbb{Z}[\![x_1, \dots, x_n]\!] \tag{3-2}$$

into the ring of formal power series in noncommuting variables $\{x_i\}$, defined by

$$M(g_i) = 1 + x_i, \quad M(g_i^{-1}) = 1 - x_i + x_i^2 - x_i^3 \pm \cdots.$$

The Magnus expansion induces a homomorphism (which abusing the notation we denote again by M) from the free Milnor group

$$M\colon MF_{g_1,\dots,g_n} \longrightarrow R_{x_1,\dots,x_n}, \tag{3-3}$$

into the quotient $R_{x_1,\dots,x_n}$ of $\mathbb{Z}[\![x_1, \dots, x_n]\!]$ by the ideal generated by all monomials $x_{i_1} \cdots x_{i_k}$ with some index occurring at least twice. It is proved in [9] that the homomorphism (3-3) is well defined and injective.

The relations in (3-1) are very well suited for studying links L in S^3 up to *link homotopy*. In this original setting for the definition of the Milnor group [9] one takes G to be the link group $\pi_1(S^3 \smallsetminus L)$ and a normal set of generators is provided by meridians m_i to the link components. Two links are link-homotopic if they are connected by a 1–parameter family of link maps where different components stay disjoint for all values of the parameter. If L, L' are link-homotopic then their Milnor groups ML, ML' are isomorphic, and moreover an n–component link L is nullhomotopic in this sense if and only if ML is isomorphic to the free Milnor group $MF_{m_1,\dots,m_n}$.

The Milnor group is also useful for studying surfaces Σ in the 4–ball which are disjoint but which may have self-intersections: in this case the Clifford tori linking the double points in D^4 give rise to the relations (3-1) in $M\pi_1(D^4 \smallsetminus \Sigma)$. The theory of link homotopy discussed above may be interpreted as the study of links up to singular concordance (links $L \subset S^3 \times \{0\}$, $L' \subset S^3 \times \{1\}$ bounding disjoint maps of annuli into $S^3 \times [0, 1]$). In particular, a link is nullhomotopic if and only if its components bound disjoint maps of disks into D^4, and in this case the Milnor group is isomorphic to the free Milnor group. Surfaces of higher genus give rise to additional relations in

the fundamental group of the complement, and the Milnor group in this more general case depends on linking of the surfaces in D^4.

3.2 The relative-slice problem

The proofs of the embedding and nonembedding statements in this paper will be based on the *relative-slice* reformulation of the problem; see [3; 6] for a more detailed introduction.

Let $L = \{l_i\}$ denote the attaching curves of the 2–handles of the 4–manifolds that are to be embedded in the 4–ball, also let $R = \{r_j\}$ denote the dotted curves corresponding to the 1–handles. The 1–handles are considered as unknotted 2–handles removed from the collar on the attaching region of a given 4–manifold. Considering a slightly smaller 4–ball (the original D^4 minus the collars on the attaching regions), a given embedding problem is then equivalent to "slicing L relative to R": finding slices for the link L in the handlebody $D^4 \cup_R 2$–handles, where the 2–handles are attached with zero-framing to D^4 along the dotted components R. (See [3; 6] for more details and illustrations.)

The relative-slice problems corresponding to the statements in Theorem 1 for the Hopf link and for the Borromean rings are shown in Figures 3 and 8 respectively. The circled numbers next to the components r_1, r_2 in Figure 3 are the indices of the slices that go over the 2–handle attached to the curves r_i; this is discussed further in Section 3.3 below.

In practice the slices in a solution to the relative-slice problem will be constructed by taking band-sums of the components l_i with parallel copies of the curves r_j. These bands correspond to index-1 critical points of the slices with respect to the radial Morse function on D^4, and parallel copies of r_j bound disjoint embedded disks in the 2–handle attached to r_j. If the resulting link L' is nullhomotopic (in the sense discussed in Section 3.1), the construction of the (singular) slices is completed by capping off the components of L' by disjoint disks in D^4. These disks in general will have self-intersections; indeed the approach outlined here can be used either to find an obstruction or to find a solution up to link homotopy, ie disjoint slices which may have self-intersections, as in Section 3.3.

The Milnor group will be used to carry out this strategy to find a solution for the Hopf link in Section 3.3 and to find an obstruction for the Borromean rings in Section 4. As indicated in Section 3.1, the Milnor group is very well suited for calculations up to link-homotopy. In both problems at hand, omitting one of the attaching curves for the 2–handles gives the unlink. Moreover, any band-sum of this unlink with parallel copies

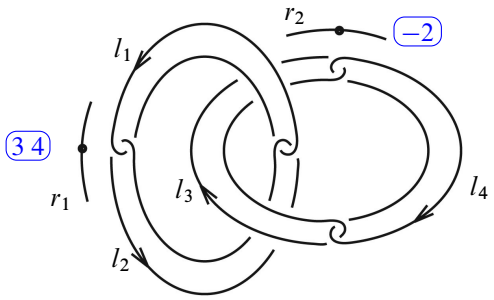

Figure 3: The relative-slice formulation of the embedding problem in D^4 for two copies of the manifold A attached to the Hopf link: the curves $l_1, \dots, l_4$ need to be sliced in the handlebody $D^4 \cup_{r_1, r_2} 0$–framed 2–handles. (Orientations of link components are used in calculations in Section 3.3.)

of the given dotted curves (taking place in the context of the relative-slice problem) yields a homotopically trivial link. Therefore the Milnor group of the complement of the resulting band-summed link is isomorphic to the free Milnor group. The problem then is reduced to the question of whether band-summing may be performed so that the omitted component is trivial in the free Milnor group (so that the entire link is homotopically trivial). A specific choice of band-sums shows that the answer is "yes" for the Hopf link, and an argument analyzing Jacobi relations in the free Milnor group proves that the answer is "no" for the Borromean rings.

Remark 3.1 Recall the requirement, introduced before the statement of Theorem 1, that the embeddings $f_i\colon (M, \gamma) \hookrightarrow (D^4, S^3)$ in the definition of M–slice are "standard": each embedding f_i is isotopic to the original embedding $(M, \gamma) \subset (D^4, S^3)$. This requirement is reflected in the relative-slice context by the condition that the slices bounded by the curves l_i of a given 4–manifold do not go over the 2–handle (attached to the dotted curve) corresponding to the 1–handle of the same 4–manifold. Specifically, in Figure 3 the slices for l_1, l_2 should not go over the 2–handle attached to r_1, and similarly l_3, l_4 should not go over r_2. (Note that without this restriction there is in fact a rather straightforward solution to this relative-slice problem.) In fact, the obstruction for the Borromean rings in Section 4 uses only a weaker consequence of this condition, that the curves l_i *homologically* do not go over the 2–handle corresponding to the 1–handle of the same 4–manifold (see Condition 4.1). One could use this to define a *homologically standard* requirement which interpolates between arbitrary embeddings and standard embeddings, and the results of this paper hold in this setting as well. (This may also serve as a bridge with the classical subject of slice links since the usual slice disks are of course "homologically standard".) This weaker homological condition on embeddings is not pursued further in the present paper since it does not

have an immediate application in the A-B slice problem which is the main motivation for the "standard" requirement.

3.3 Proof of Theorem 1 for the Hopf link

Consider the relative-slice setup in Figure 3, where the dotted curves are defined in Figure 2. To read off the word represented by l_1 in $M\pi_1(S^3 \smallsetminus (l_2 \cup l_3 \cup l_4 \cup r_1 \cup r_2))$ it is useful to consider a 2–stage capped grope (see Freedman and Quinn [4]) shown in Figure 4 bounded by l_1: the two surface stages are embedded in the link complement while the caps intersect the link as shown in Figure 4. (There are several versions of *gropes* considered in the literature. Throughout this section the term "grope" refers to *half-gropes*; see [3, Definition 2.4 and Figure 2.1].)

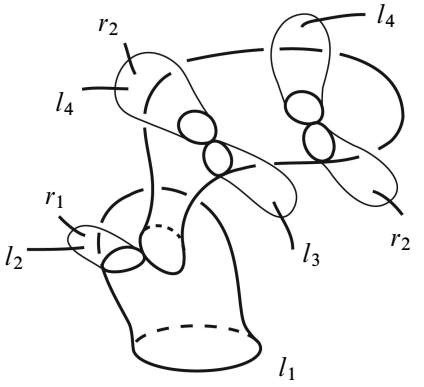

Figure 4: A 2–stage capped grope bounded by l_1 in Figure 3

A more detailed construction of this grope is shown in Figure 5. Specifically, the link in Figure 3 is a *composition* (in the sense of [3, Theorem 2.3]) of the two links shown in Figure 5. Considering the standard genus-one Heegaard decomposition of S^3, the components l_1, l_2, r_1 may be thought of as being contained in one of the solid tori, and the components l_3, l_4, r_2 are in the other solid torus of the decomposition. The first solid torus is pictured on the left in Figure 5 as the complement of the dotted curve. The (genus-one) first stage surface of the grope is shown in that figure. One cap for that surface intersects the components l_2, r_1. There is another cap, intersecting the dotted curve, visible in the picture. The second stage is obtained by removing a small meridional disk from this cap. The resulting boundary component is then filled in by the genus-two surface bounded by the curve Λ in the complement of the link in Figure 5 on the right.

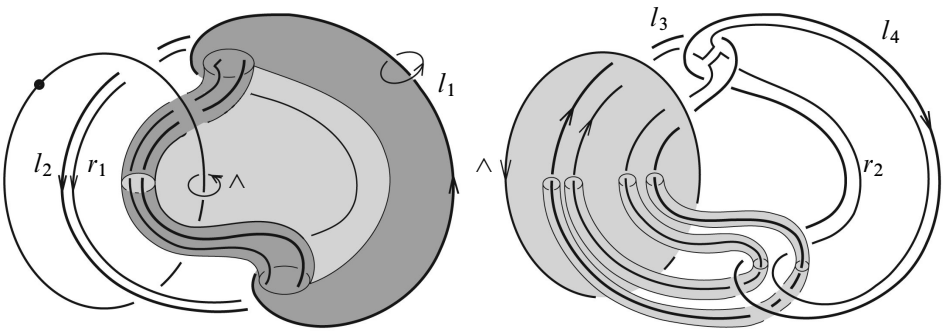

Figure 5: A more detailed construction of the grope in Figure 4: for clarity of illustration the part of the curve r_1 located behind the surface in the figure on the left is not shown (compare with Figure 2).

The component l_1 is seen to be represented by the word

$$l_1 = [[m_3, m_4 \cdot b] \cdot [b, m_4], m_2 \cdot a], \tag{3-4}$$

where m_i, a, b denote meridians to l_i, r_1, r_2 respectively. Recall that meridians are small circles linking the components, connected by arcs to the basepoint. The meridians, viewed as elements of the fundamental group of the link, depend on the choice of these arcs, as well as on the choice of the orientations of the small circles. It will be clear from the proof below that the choice of connecting arcs (and the choice of bands) is not going to be important for the argument since the difference between various choices is measured by higher-order commutators which are trivial in the relevant Milnor group.

To fix the ambiguity with orientations, consider the orientations of the link components specified in Figure 5 (also see Figure 3). Orient the meridians using the "right-hand rule", so the linking number of each component with its meridian is $+1$, as illustrated for l_1 in Figure 5. A direct calculation shows that the exponents of all meridians in (3-4) are $+1$. It is worth mentioning that the techniques developed for the proof of Theorem 1 in this paper, both for the Hopf link and for the Borromean rings, are quite robust. They work for a family of examples generalizing the main example in Figure 2. For instance, the proof goes through if the band visible in the definition of the dotted curve in Figure 2 were twisted. In this case the exponents of the two meridians labeled b in (3-4) would have been opposite.

Consider band-sums indicated in Figure 3: the circled numbers are the indices of the slices (bounded by the curves l_i) that go over the 2–handles attached to r_1, r_2. Specifically, add one parallel copy of r_1 to both l_3 and l_4, and add a parallel copy of r_2 with reversed orientation to l_2. Denote the components formed by the band-summing by l_1', l_2', l_3', l_4'. (l_1' equals l_1 since no band-summing is performed on this component.)

Proposition 3.2 *The link (l_2', l_3', l_4') is homotopically trivial.*

Proof A useful tool is the *half-grope lemma* [3, Theorem 2.5] (also see [5, Theorem 2] for a streamlined proof). It states that if the components of an n–component link bound disjoint maps of $(n-1)$–stage gropes in D^4 then the link is homotopically trivial. Therefore in our context it suffices to find disjoint maps of three 2–stage gropes into D^4, bounded by l_2', l_3', l_4'. Consider two parallel copies of r_1 in Figure 3 (without band-summing them with l_3, l_4). Recall the detailed drawing of the handle diagram in the solid torus in Figure 2. Since l_1 is missing from the link currently under consideration, observe that these two parallel copies of r_1 are isotopic within the solid torus to the curves labeled $\overline{3}, \overline{4}$ in Figure 6.

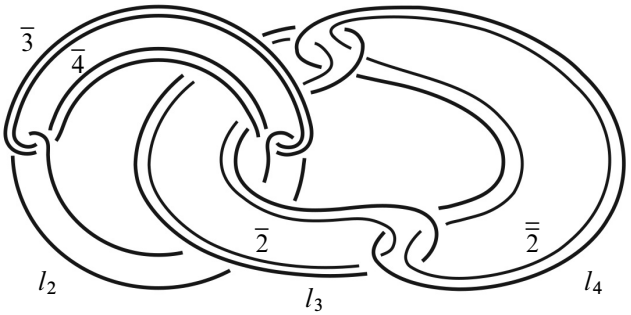

Figure 6

Consider the 7–component link in Figure 6. The curve l_2 bounds an embedded 2–stage grope, which can be easily located in the picture, in the complement of the other components in S^3. Extend these other 6 components by a product in the collar $S^3 \times [0, \epsilon]$ in D^4. Since l_2 is not present in $S^3 \times \{\epsilon\}$, the 6 components form the unlink and so bound disjoint disks in $S^3 \times \{\epsilon\}$. Therefore the 7–component link in Figure 6 bounds disjoint 2–stage gropes in D^4. (By definition the disk is an n–stage grope, for any n.) The link (l_2', l_3', l_4') is formed from the link in Figure 6 by band-summing l_3 with the curve labeled $\overline{3}$, l_4 with $\overline{4}$, and also l_2 with $\overline{2}$ and $\overline{\overline{2}}$. Taking a boundary-connected sum of the 2–stage gropes constructed above along the bands defining the band-sums yields three disjoint 2–stage gropes in D^4, bounded by l_2', l_3', l_4'. The half-grope lemma completes the proof of Proposition 3.2. □

Recall the commutator identities (cf Magnus, Karrass and Solitar [8, Theorem 5.1])

$$[x, yz] = [x, z][x, y]^z, \quad [xz, y] = [x, y]^z [z, y]. \tag{3-5}$$

We will now take a brief digression to discuss a basic fact, important for the argument here and in Section 4, that conjugation in the commutator identities (3-5) and (3-7)

below does not affect calculations in the Milnor group in our setting. The same comment applies to conjugation that results from different choices of basepoints. The key point is that the component l_1 is in the third term of the lower central series of $\pi_1(S^3 \smallsetminus (l_2' \cup l_3' \cup l_4'))$. Geometrically this is reflected in the fact that it bounds a two-stage grope in Figure 4; this may be seen algebraically using the expression (3-4) and the identities (3-5). Recall from Section 3.1 that the Magnus expansion M of the free Milnor group $M\pi_1(S^3 \smallsetminus (l_2' \cup l_3' \cup l_4'))$ into the ring R_{x_2,x_3,x_4} is well defined and injective. The Magnus expansion takes any element of the third term of the lower central series to a polynomial of the form $1+$(some linear combination of monomials of length 3 in nonrepeating variables x_2, x_3, x_4). The effect of conjugation on the Magnus expansion is the addition of higher order monomials. However since the monomials in the expansion $M(l_1)$ are already of maximal length in R_{x_2,x_3,x_4}, any type of conjugation mentioned above does not change $M(l_1)$. Since M is injective, the element represented by l_1 in $M\pi_1(S^3 \smallsetminus (l_2' \cup l_3' \cup l_4'))$ is also unchanged by conjugation. An alternative argument for this fact, not using the Magnus expansion, may be given by directly using the defining Milnor relation (3-1).

The band-summing (indicated in Figure 3) defining the link (l_1', l_2', l_3', l_4') results in substitutions $a = m_3 m_4$ and $b = m_2^{-1}$ in (3-4). Disregarding conjugation in (3-5) and collecting commutators with distinct indices, one has

$$\begin{aligned} (3\text{-}6)\quad l_1 &= [[m_3, m_4 \cdot m_2^{-1}] \cdot [m_2^{-1}, m_4], m_2 \cdot m_3 \cdot m_4] \\ &= [[m_3, m_4], m_2] \cdot [[m_3, m_2^{-1}], m_4] \cdot [[m_2^{-1}, m_4], m_3]. \end{aligned}$$

Using the identity $[x^{-1}, y] = [y, x]^{x^{-1}}$ (where conjugation is again irrelevant), l_1 equals

$$[[m_3, m_4], m_2] \cdot [[m_2, m_3], m_4] \cdot [[m_4, m_2], m_3].$$

Omitting conjugation in the Hall–Witt identity [8, Theorem 5.1]

$$(3\text{-}7) \qquad [[x, y], z^x] \cdot [[z, x], y^z] \cdot [[y, z], x^y] = 1,$$

one gets the Jacobi relation

$$(3\text{-}8) \qquad [[x, y], z] \cdot [[z, x], y] \cdot [[y, z], x] = 1,$$

establishing that $l_1 = 1 \in MF_{m_2,m_3,m_4}$.

Recall from Proposition 3.2 that the link (l_2', l_3', l_4') is homotopically trivial. The point of the calculation above is that $l_1 = 1 \in M\pi_1(S^3 \smallsetminus (l_2' \cup l_3' \cup l_4')) \cong MF_{m_2,m_3,m_4}$. Therefore it follows from [9, Theorem 3] that $L' = (l_1, l_2', l_3', l_4')$ is homotopically trivial and so its components bound disjoint maps of disks into D^4. This gives a

solution up to link-homotopy to the relative-slice problem for the Hopf link which is "standard" in the sense of Remark 3.1.

Remark 3.3 To illustrate the subtlety of the problem for the Hopf link analyzed above, it is interesting to note that while a link-homotopy solution is shown to exist for the relative-slice problem in Figure 3, there are no *embedded* slices for the components $l_1, \dots, l_4$ in this problem. This may be proved by finding an obstruction similar to that in [7] for a link obtained by handle slides on the link $(l_1, \dots, l_4)$. The condition of being relatively slice is preserved by handle slides but the condition of being relatively slice up to link homotopy is not preserved in general.

3.4 Completion of the construction of M

The detail that is missing from the conclusion of the proof of Theorem 1 for the Hopf link is that the two copies of the manifold M have to be *embedded*, while the outcome of the argument so far is a map of two copies A_1, A_2 of A into D^4 where individual 2–handles have self-plumbings. (Moreover, as discussed in the introduction the embeddings are required to be isotopic to the original embedding $M \subset D^4$.) The nullhomotopies produced as a result of Milnor group calculations may be realized as a sequence of standard "elementary homotopies" of link components. The manifold M will be defined to be A with a number of self-plumbings of its two 2–handles, determined by those of both A_1 and A_2.

The precise details of the construction of M are as follows. It is worth mentioning right away that the *standard* condition is imposed on each individual embedding of M. That is, after M is constructed two copies of it will be disjointly embedded with their attaching circles corresponding to the two components of the Hopf link, and the embedding of each copy will be shown to be standard after the other component is disregarded. Figure 7 is a concise illustration of the construction.

Each of the two links (l_1, l_2, r_2) and (l_3, l_4, r_1) is a three-component unlink, and band sums in the proof above may be easily found so that both (l_1', l_2'), (l_3', l_4') are two-component unlinks. Taking a band-sum of l_2 with r_2 and capping off with the core of the 2–handle attached to r_2 amounts to a $(1,2)$–pair of critical points of the slice for l_2 with respect to the radial Morse function on D^4. (This Morse function is considered on the original 4–ball which contains the 2–handles attached along r_1, r_2 and into which the manifolds A_1, A_2 are embedded; see the second paragraph of Section 3.2. The slightly smaller 4–ball where the relative-slice problem is being considered is obtained by removing the collars on the attaching regions of A_1, A_2.) Since (l_1, l_2, r_2) is the unlink, this pair of critical points can be canceled and (ignoring the components l_3, l_4)

the result is an isotopy of (l_1, l_2) in $S^3 \times I$. (Compare with [6, Figure 15].) Similarly, (considering just the last two components) band-summing l_3 and l_4 with copies of r_1 may be realized instead as an isotopy of l_3, l_4.

We summarize the setup: the 4–component link $L' := (l'_1, \dots, l'_4)$ is nullhomotopic, and the two-component sublinks $(l'_1, l'_2), (l'_3, l'_4)$ are individually unlinks. We will next construct specific nullhomotopies of the components of L'. Start with any link homotopy from L' to the 4–component unlink. Rather than capping them off by disks right away, let the first two components move by an isotopy away from the last two components. For reasons which will be clear below, next we run the entire link-homotopy of l'_3, l'_4 backwards, while the first two components stay fixed as unknots away from l'_3, l'_4. The result is a 4–component unlink which may be capped off by disks. Denote the resulting link homotopies (disjoint annuli with self-intersections) of l'_1, l'_2 by H and l'_3, l'_4 by H'; see the diagram on the left in Figure 7. To prepare for the following step of the construction, note that both H, H' are level-preserving singular maps $(S^1 \sqcup S^1) \times [0,1] \longrightarrow S^3 \times [0,1]$ giving two-component unlinks at times $0, 1$. Their singularities consist of finitely many double point self-intersections, and they are isotopies when restricted to subintervals of $[0,1]$ not containing singular points. Although H' is defined using l'_3, l'_4, it can be "applied" to any two-component unlink in $S^3 \times \{0\}$, for example to l'_1, l'_2.

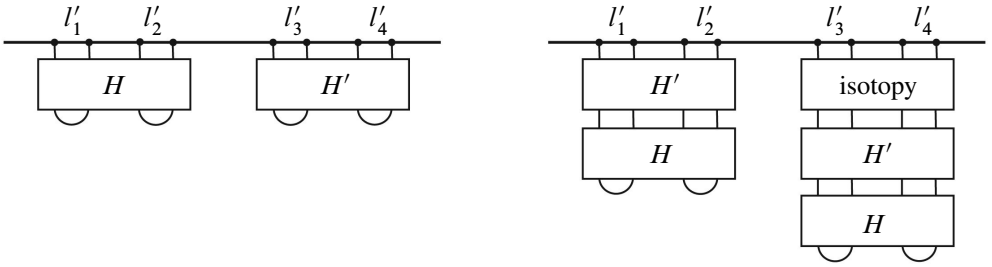

Figure 7: A schematic picture of a preliminary link-homotopy of L (left) and of a modified link homotopy (right) yielding two disjoint standard embeddings of M. The horizontal direction depicts S^3 and the vertical direction corresponds to the radial coordinate in D^4. The link components l'_i are pictured as 0–spheres in $S^3 = \partial D^4$. Each box H, H' denotes two disjoint level-preserving annuli, possibly with self-intersections. The top and the bottom of each of H, H' individually is a two-component unlink.

The result so far is insufficient for the definition of M since H, H' may be nonisotopic in D^4. A suitable link-homotopy of L' is constructed instead as follows. As shown on the right in Figure 7, as a preliminary step start by applying the link homotopy H' to the components l'_1, l'_2, while letting l'_3, l'_4 move by an isotopy in their complement. More

precisely, recall from the previous paragraph that H' is a level-preserving map $(S^1 \sqcup S^1)\times I \longrightarrow S^3\times I$ which is an isotopy at generic times and whose singularities consist of double point self-intersections at finitely many times. Given two components, l'_3 and l'_4, in the complement of l'_1, l'_2 in $S^3 \times \{0\}$, there exists an isotopy moving them in the complement of H': a level-preserving embedding $(S^1\sqcup S^1)\times I \hookrightarrow S^3\times I \smallsetminus \text{image}(H')$. Indeed, each double point of H' is described by a movie where two strands of either l'_1 or l'_2 move by an isotopy in S^3 and intersect in a single point. By general position, since l'_3, l'_4 are 1–dimensional submanifolds of S^3, they may be kept disjoint from H' during this movie. This completes the argument for the existence of an isotopy of l'_3, l'_4 in the complement of H'.

Since H' was constructed as a link-homotopy followed by its reverse, the outcome of the previous paragraph is an identical copy of $L' = (l'_1, \dots, l'_4)$. Now run the link-homotopy H, H' of L'. The result is a 4–component unlink. Cap off the first two components with disks and apply H to the 3rd and 4th components. Finally, cap off the last two components. Now the nullhomotopy of (l'_1, l'_2) is isotopic to the nullhomotopy of (l'_3, l'_4): up to isotopy each one is H' followed by H and then capped off with standard disks, Figure 7. Define M to be either of the two embeddings of the manifold A in Figure 2 with self-plumbings of the 2–handles constructed above. This yields an embedding of two standard copies of M as required in the part of Theorem 1 concerning the Hopf link.

4 An obstruction for the Borromean rings

This section completes the proof of Theorem 1 by showing that the Borromean rings do not bound disjoint standard embeddings of three copies of (M, γ) in D^4. This argument is important in the context of the A-B slice problem, discussed in Section 5.

The relative-slice formulation corresponding to the embedding problem for three copies of the manifold A in Section 2 is shown in Figure 8. (The manifold M in the statement of Theorem 1 was defined in Section 3.4 as A with a number of self-plumbings of its 2–handles. As noted in Section 3.1 these self-plumbings do not affect the Milnor group arguments given below.)

Suppose to the contrary that the Borromean rings bound disjoint standard embeddings of three copies A_i, $i = 1, 2, 3$ of A; equivalently assume the link in Figure 8 is relatively slice, subject to the "standard" condition discussed in Remark 3.1. We specify a weak consequence of this condition, sufficient for the proof of Theorem 1 for the Borromean rings:

Condition 4.1 The slices for l_1, l_2 do not homologically go over the 2–handle attached to r_1, and similarly l_3, l_4 do not go over r_2, and l_5, l_6 do not go over r_3. Here, a slice *does not homologically go over a 2–handle* if its ($\mathbb{Z}$–valued) algebraic intersection number with the cocore of the 2–handle is zero.

It will be shown that the components l_i do not bound disjoint singular disks subject to this restriction. (Without this restriction, it is not hard to find a solution to this relative-slice problem.) This condition is important in the A-B slice problem [3]; see Section 5.

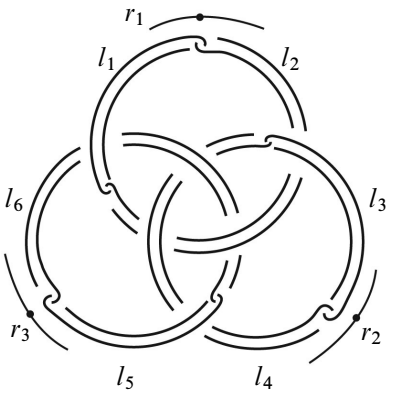

Figure 8: The relative-slice problem for embedding three copies of A on the Borromean rings: do the components $l_1, \dots, l_6$ bound disjoint disks in $D^4 \cup_{r_1,r_2,r_3}$ 2–handles? The dotted curves r_1, r_2, r_3 are shown only schematically, as explained in Figure 2.

Consider the 120–dimensional vector space V over $\mathbb{Q}$, formally spanned by all commutators of the form $[m_{i_1}, [m_{i_2}, [m_{i_3}, [m_{i_4}, m_{i_5}]]]]$ in five nonrepeating variables, so the indices $(i_1, i_2, i_3, i_4, i_5)$ range over all permutations of $\{2, \dots, 6\}$. Omitting the curves r_1, r_2, r_3 in Figure 8, the remaining link is the Bing double of the Borromean rings. Using the orientations in Figure 8 and the corresponding choice of meridians (discussed in Section 3.3), one checks the component l_1 represents the commutator

$$l_1 = [m_2, [[m_3, m_4], [m_5, m_6]]] \tag{4-1}$$

in the complement of the other five components $l_2, \dots, l_6$. An observation important for the proof below is that any band-sum of the curves $\{l_i\}$ and parallel copies of the dotted curves r_j in the link in Figure 8 gives rise to (products of) commutators of the form

$$[m_{i_1}, [[m_{i_2}, m_{i_3}], [m_{i_4}, m_{i_5}]]] \tag{4-2}$$

where $i_1, \dots, i_5$ is a permutation of $\{2, \dots, 6\}$; see Figure 9. Any such commutator is equivalent under antisymmetry relation applied to $[[m_{i_2}, m_{i_3}], [m_{i_4}, m_{i_5}]]$ to one of 15 that appear in the statement of Lemma 4.3 below. Let U be the subspace of V generated by these 15 commutators. Denote by J the subspace of V spanned by the Jacobi and anticommutation relations.

Remark 4.1 Let F denote the free group $F_{m_2,\dots,m_6}$. The quotient V/J is isomorphic to $(MF)^5 \otimes \mathbb{Q}$, where $(MF)^5$ denotes the 5^{th} term of the lower central series of the Milnor group MF.

Remark 4.2 The notation will alternate between the *product* of commutators, considered in the Milnor group MF and the *sum* of commutators considered in the abelian group $(MF)^5$. (Note that $(MF)^6$ is trivial.) This should not cause any confusion.

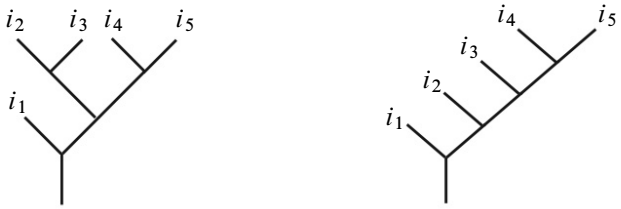

Figure 9: The tree on the left encodes the bracketing in the commutators of the form $[m_{i_1}, [[m_{i_2}, m_{i_3}], [m_{i_4}, m_{i_5}]]]$ arising in the link in Figure 8, and the tree on the right encodes commutators $[m_{i_1}, [m_{i_2}, [m_{i_3}, [m_{i_4}, m_{i_5}]]]]$ spanning the vector space V.

Lemma 4.3 *The intersection $U \cap J$ is a 1–dimensional subspace of V spanned by the product of 15 commutators:*

$$
\begin{aligned}
w := \; & [m_2, [[m_3, m_4], [m_5, m_6]]] \cdot [m_2, [[m_5, m_3], [m_4, m_6]]] \cdot [m_2, [[m_4, m_5], [m_3, m_6]]] \\
& \cdot [m_3, [[m_4, m_2], [m_5, m_6]]] \cdot [m_3, [[m_2, m_5], [m_4, m_6]]] \cdot [m_3, [[m_5, m_4], [m_2, m_6]]] \\
& \cdot [m_4, [[m_2, m_3], [m_5, m_6]]] \cdot [m_4, [[m_5, m_2], [m_3, m_6]]] \cdot [m_4, [[m_3, m_5], [m_2, m_6]]] \\
& \cdot [m_5, [[m_3, m_2], [m_4, m_6]]] \cdot [m_5, [[m_2, m_4], [m_3, m_6]]] \cdot [m_5, [[m_3, m_4], [m_2, m_6]]] \\
& \cdot [m_6, [[m_2, m_3], [m_4, m_5]]] \cdot [m_6, [[m_4, m_2], [m_3, m_5]]] \cdot [m_6, [[m_2, m_5], [m_3, m_4]]].
\end{aligned}
$$

Therefore $\dim(U/(J \cap U)) = 14$.

The element w is certainly in U; an explicit calculation in Appendix A.1 using the Jacobi relations (3-8) shows that w is also in J.

The following proposition describes a convenient basis of the space of commutators in nonrepeating variables modulo the Jacobi and antisymmetry relations. (A directly analogous statement works for n–fold commutators for arbitrary n; the result is stated below in the case $n = 5$ relevant for the current proof.) Of course the index "6" in the statement below can be replaced by any fixed index in $\{2, \dots, 6\}$. The proof of Lemma 4.3 will follow from the following proposition.

Proposition 4.4 *The collection of commutators of the form*

$$[m_{i_1}, [m_{i_2}, [m_{i_3}, [m_{i_4}, m_6]]]],$$

where the right-most index is 6 *and* $i_1, \dots, i_4$ *range over all permutations of* $2, \dots, 5$, *forms a basis of* V/J.

Proof To show that the commutators in the statement span V/J, start with any commutator $[m_{i_1}, [m_{i_2}, [m_{i_3}, [m_{i_4}, m_{i_5}]]]]$ and use the antisymmetry relation to shift m_5 to the right-most position. In general this will change the bracketing pattern of the commutator. Now the Jacobi relations (3-8) may be used to rebracket and get a product of commutators of the form

$$[m_{i_1}, [m_{i_2}, [m_{i_3}, [m_{i_4}, m_6]]]]. \tag{4-3}$$

To show that these elements are linearly independent in V/J, consider the Magnus expansion (3-3) and note that the monomial $x_{i_1}x_{i_2}x_{i_3}x_{i_4}x_6$ is present only in the Magnus expansion of the commutator $[m_{i_1}, [m_{i_2}, [m_{i_3}, [m_{i_4}, m_6]]]]$. □

Proof of Lemma 4.3 It follows from Proposition 4.4 that V/J is 24–dimensional. Recall that U is a 15–dimensional subspace of V spanned by the commutators that appear in the statement of Lemma 4.3. Using the Jacobi and antisymmetry relations, 12 among these 15 commutators are seen to be products of two "basic" commutators (4-3). In total these $24 = 12 \cdot 2$ basic commutators form the basis of V/J and so clearly no linear combination of the first 12 commutators listed in Lemma 4.3 may intersect J nontrivially. There are also 3 "complicated" commutators which appear last in Lemma 4.3. Each of them is a product of 8 commutators of the form (4-3), see Appendix A.1, and the total $24 = 8 \cdot 3$ of them again are a basis of V/J. There is only one nontrivial linear combination among the 15 commutators, the one stated in the lemma. □

To conclude the proof that the link in Figure 8 is not relatively slice, recall from (4-1) that without the components $\{r_j\}$ the curve l_1 reads off the first commutator in the definition of w in Lemma 4.3. Let w' denote the rest of them, so $w = [m_2, [[m_3, m_4], [m_5, m_6]]] \cdot w'$. Then for the relative-slice problem in Figure 8 to have a solution, the slices going over r_1, r_2, r_3 must "account for" the product w'.

Proposition 4.5 *The element w' cannot be realized by band-sums of the relative-slice problem in Figure 8.*

The proof of this proposition consists of an explicit check that the corresponding system of equations does not have a solution. In this problem there are 14 equations of degrees 2 and 3 in 12 variables, explicitly written down in the Appendix; see Appendix A.2. The fact that there are no integral solutions is verified using Mathematica (Section A.3), although using symmetries of the equations it is in fact possible to check this fact by hand. It is interesting to note that there are *rational* solutions which do not seem to have a geometric interpretation in the context of the relative-slice problem.

It is instructive to compare Proposition 4.5 with Section 5.2 and Figure 13 where a solution is shown to exist for a closely related problem.

We summarize the argument proving Theorem 1 for the Borromean rings. Suppose there exist disjoint standard embeddings of three copies of the manifold M bounded by the Borromean rings. Therefore there exists a solution to the relative-slice problem in Figure 8, subject to Condition 4.1. Then, as discussed in Section 3.2, there exist band-sums of the components $l_1,\dots,l_6$ with parallel copies of r_1, r_2, r_3 (again subject to Condition 4.1) such that the resulting link $(l'_1,\dots,l'_6)$ is homotopically trivial. A direct generalization of Proposition 3.2 shows that for any such band-sum, omitting the first component, the rest of the link $(l'_2,\dots,l'_6)$ is homotopically trivial. Proposition 4.5 implies that for any band-sum, l'_1 is nontrivial in $M\pi_1(S^3\smallsetminus(l'_2,\dots,l'_6))\cong MF_{2,\dots,6}$. Therefore for any band-sum the link $(l'_1,\dots,l'_6)$ is not nullhomotopic. This contradiction concludes the proof of Theorem 1.

Remark 4.6 An alternative to converting slices into band-sums is to use the Milnor group of the 4–manifold $X^4 := D^4\cup_{r_1,r_2,r_3}$ 2–handles$\smallsetminus$(slices for $l_1,\dots,l_6$); see [7, Section 4]. The Milnor group calculations in the proof of Theorem 1 in both contexts are identical.

5 The A-B slice problem

5.1 Analysis of the decomposition $D^4 = A\cup B$

Consider the complement of the manifold A in Figure 2, $B = D^4\smallsetminus A$. A handle decomposition for B (with the attaching curve β) may be obtained from that of A by exchanging the 1– and 2–handles as explained in [3]; see Figure 10. The question relevant from the perspective of the A-B slice problem is whether the Borromean rings bound disjoint embeddings of three copies of A, and also disjoint embeddings

of three copies of B where the embeddings are all *standard*; see Remark 3.1. (The origin of the "standard" condition on embeddings is in the formulation of the A-B slice problem [1; 3]: it reflects the covering group action on the 4–ball, which is predicted by the 4–dimensional topological surgery conjecture.)

It was proved in Section 4 that there are no disjoint embeddings of three copies of A. We will next examine the embedding problem for three copies of B with the boundary condition given by the Borromean rings. It is worth noting that the Hopf link is not B–slice. Observe in Figure 10 that the attaching curve β bounds a surface in B. Therefore the nontriviality of the linking number of the Hopf link implies that its components do not bound disjoint copies of B. In fact, this argument immediately generalizes to show that the Hopf link is not A-B–slice: the attaching curve of one of the two sides of any decomposition $D^4 = A \cup B$ bounds rationally. Therefore the linking number is an obstruction. The interested reader will find related in-depth discussion in [2].

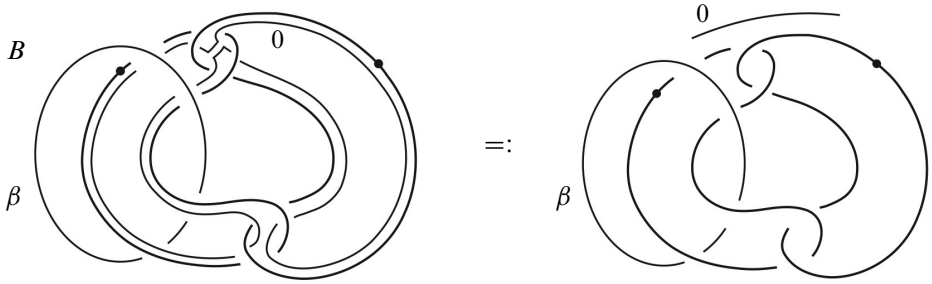

Figure 10: A Kirby diagram of the 4–manifold $B = D^4 \smallsetminus A$. As in Figure 2, the picture on the right will serve as a short-hand notation for B.

As in Section 4 the embedding question for the Borromean rings is reformulated as a relative-slice problem, shown in Figure 11. The problem is to find disjoint disks (possibly with self-intersections) for the link components labeled $1-6$ in the handlebody $D^4 \cup$ six zero-framed 2–handles attached along the dotted curves. The sought solution has to satisfy the *standard* assumption discussed in Remark 3.1. This means that the slices for l_1, l_4 are not allowed to go over the two 2–handles attached to the dotted curve on the upper left, and similarly l_2, l_5 should not go over the two 2–handles on the right, and l_3, l_6 should not go over the 2–handles on the lower left.

The circled indices next to the dotted component in Figure 11 indicate band-sums such that all $\bar{\mu}$–invariants of the resulting link of length less than or equal to 3 vanish. The original obstruction for the Borromean rings, $\bar{\mu}_{123}$, is of length 3, so the "primary" obstruction is killed. To find a link-homotopy solution to this relative-slice problem

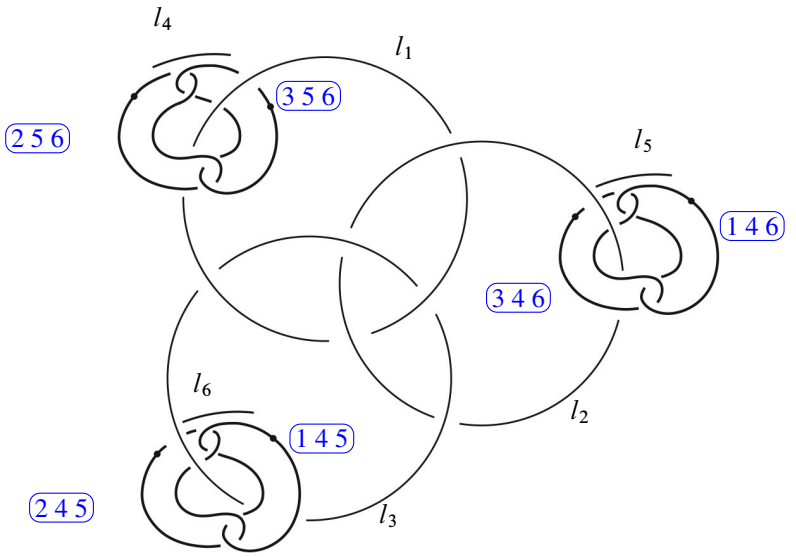

Figure 11: The relative-slice problem for three copies of B (Figure 10) on the Borromean rings

one needs all $\overline{\mu}$–invariants up to order 6 to be zero. Unlike the settings in Sections 3 and 4, conjugation corresponding to the choice of meridians and bands is important here. It seems likely that a careful choice of bands should give rise to a link homotopy solution, but at present this is an open question.

5.2 An obstruction for a family of examples

Consider the submanifolds $A', A'' \subset D^4$ shown in Figure 12, closely related to the submanifold A constructed in Section 2, and consider the corresponding decompositions $D^4 = A' \cup B'$, $D^4 = A'' \cup B''$.

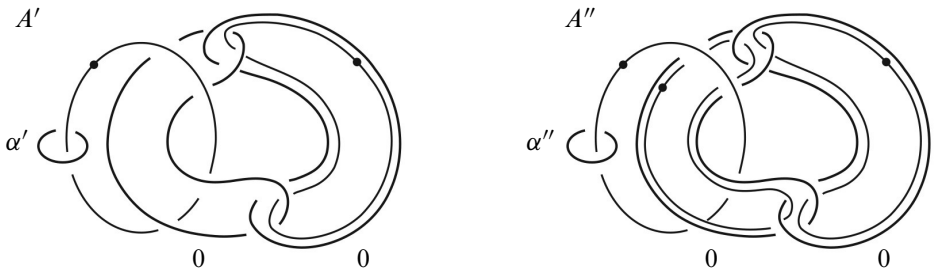

Figure 12: Two variations of the example from Section 2

A solution up to link-homotopy to the relative-slice problem for three copies of A'' on the Borromean rings is given in Figure 13. (Note the asymmetry of labels going over the top two components: some assymetry is necessary since a solution does not exist for three copies of A, according to Theorem 1.) The reader is encouraged to check that the resulting product of commutators representing l_6 in nonrepeating variables indeed equals the element w from Lemma 4.3. It is not difficult to check using $\bar{\mu}_{123}$ that the Borromean rings do not support standard embeddings of three copies of the other side of this decomposition, B''.

The decomposition $D^4 = A' \cup B'$ was the subject of the papers [6; 7]. It is shown in [7] that the Borromean rings do not bound three standard copies of A'.

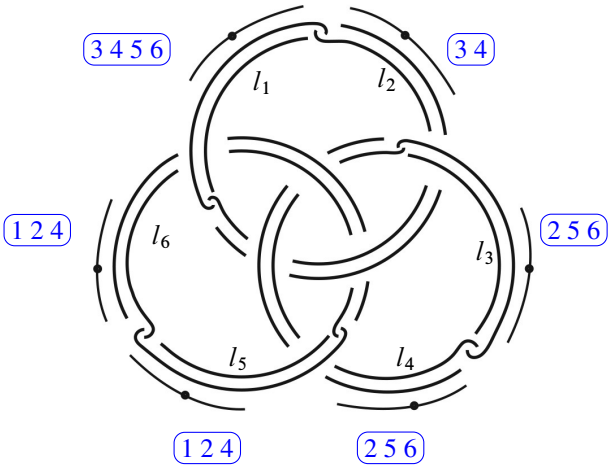

Figure 13: The dotted curves of three copies of A'' are shown only schematically (see the Kirby diagram on the right in Figure 12). The circled indices show how the components $l_1, \dots, l_6$ go over the 2–handles attached to the dotted curves, yielding the element w from Lemma 4.3 and therefore solving the relative-slice problem up to link-homotopy.

5.3 Summary

Given a decomposition of the 4–ball, $D^4 = A \cup B$, into two codimension-zero submanifolds where the "attaching curves" α, β of A, B form the Hopf link in $S^3 = \partial D^4$, an important question in the A-B slice program is to determine whether there is necessarily an obstruction to the Borromean rings being both A–slice and B–slice in the sense of Theorem 1. The side which carries an obstruction (if there is one) is called "strong"; see [3; 6; 7]. The goal is to determine a strong side for any decomposition $D^4 = A \cup B$.

To summarize the results of this paper in the context of the A-B slice problem, in each of the examples considered here, $D^4 = A \cup B = A' \cup B' = A'' \cup B''$ (Figures 2 and 12), one of the two sides is found to be "strong". A novel type of an obstruction is used here: the key to deciding which side is strong is whether the element w in Lemma 4.3 is in the image of the relator curves on the relevant (in our notation, A)–side. The work presented here admits an immediate generalization giving rise to an obstruction for an infinite family of decompositions by further Bing doubling the links describing the Kirby diagrams in Figures 2 and 12.

Appendix: Detailed calculations

A.1 A detailed commutator list for the proof of Lemma 4.3

To verify the element w in Lemma 4.3 is in the subspace $J \subset V$, in other words that w is trivial modulo the Jacobi and antisymmetry relations, listed below is an expression of each commutator in the definition of w as a linear combination of the commutators forming the basis of V/J in Proposition 4.4. This list also makes it clear that the dimension of $U \cap J$ in the statement of Lemma 4.3 is precisely 1 (and not greater):

$$[m_2,[[m_3,m_4],[m_5,m_6]]] = [m_2,[m_3,[m_4,[m_5,m_6]]]] - [m_2,[m_4,[m_3,[m_5,m_6]]]],$$
$$[m_2,[[m_5,m_3],[m_4,m_6]]] = [m_2,[m_5,[m_3,[m_4,m_6]]]] - [m_2,[m_3,[m_5,[m_4,m_6]]]],$$
$$[m_2,[[m_4,m_5],[m_3,m_6]]] = [m_2,[m_4,[m_5,[m_3,m_6]]]] - [m_2,[m_5,[m_4,[m_3,m_6]]]],$$
$$[m_3,[[m_4,m_2],[m_5,m_6]]] = [m_3,[m_4,[m_2,[m_5,m_6]]]] - [m_3,[m_2,[m_4,[m_5,m_6]]]],$$
$$[m_3,[[m_2,m_5],[m_4,m_6]]] = [m_3,[m_2,[m_5,[m_4,m_6]]]] - [m_3,[m_5,[m_2,[m_4,m_6]]]],$$
$$[m_3,[[m_5,m_4],[m_2,m_6]]] = [m_3,[m_5,[m_4,[m_2,m_6]]]] - [m_3,[m_4,[m_5,[m_2,m_6]]]],$$
$$[m_4,[[m_2,m_3],[m_5,m_6]]] = [m_4,[m_2,[m_3,[m_5,m_6]]]] - [m_4,[m_3,[m_2,[m_5,m_6]]]],$$
$$[m_4,[[m_5,m_2],[m_3,m_6]]] = [m_4,[m_5,[m_2,[m_3,m_6]]]] - [m_4,[m_2,[m_5,[m_3,m_6]]]],$$
$$[m_4,[[m_3,m_5],[m_2,m_6]]] = [m_4,[m_3,[m_5,[m_2,m_6]]]] - [m_4,[m_5,[m_3,[m_2,m_6]]]],$$
$$[m_5,[[m_3,m_2],[m_4,m_6]]] = [m_5,[m_3,[m_2,[m_4,m_6]]]] - [m_5,[m_2,[m_3,[m_4,m_6]]]],$$
$$[m_5,[[m_2,m_4],[m_3,m_6]]] = [m_5,[m_2,[m_4,[m_3,m_6]]]] - [m_5,[m_4,[m_2,[m_3,m_6]]]],$$
$$[m_5,[[m_3,m_4],[m_2,m_6]]] = [m_5,[m_4,[m_3,[m_2,m_6]]]] - [m_5,[m_3,[m_4,[m_2,m_6]]]],$$
$$[m_6,[[m_2,m_3],[m_4,m_5]]] = [m_4,[m_5,[m_3,[m_2,m_6]]]] - [m_5,[m_4,[m_3,[m_2,m_6]]]] - [m_4,[m_5,[m_2,[m_3,m_6]]]] + [m_5,[m_4,[m_2,[m_3,m_6]]]]$$

$$+[m_2,[m_3,[m_5,[m_4,m_6]]]]-[m_3,[m_2,[m_5,[m_4,m_6]]]]$$
$$-[m_2,[m_3,[m_4,[m_5,m_6]]]]+[m_3,[m_2,[m_4,[m_5,m_6]]]],$$

$$[m_6,[[m_4,m_2],[m_3,m_5]]] = [m_3,[m_5,[m_2,[m_4,m_6]]]]-[m_5,[m_3,[m_2,[m_4,m_6]]]]$$
$$-[m_3,[m_5,[m_4,[m_2,m_6]]]]+[m_5,[m_3,[m_4,[m_2,m_6]]]]$$
$$+[m_4,[m_2,[m_5,[m_3,m_6]]]]-[m_2,[m_4,[m_5,[m_3,m_6]]]]$$
$$-[m_4,[m_2,[m_3,[m_5,m_6]]]]+[m_2,[m_4,[m_3,[m_5,m_6]]]],$$

$$[m_6,[[m_2,m_5],[m_3,m_4]]] = [m_3,[m_4,[m_5,[m_2,m_6]]]]-[m_4,[m_3,[m_5,[m_2,m_6]]]]$$
$$-[m_3,[m_4,[m_2,[m_5,m_6]]]]+[m_4,[m_3,[m_2,[m_5,m_6]]]]$$
$$+[m_2,[m_5,[m_4,[m_3,m_6]]]]-[m_5,[m_2,[m_4,[m_3,m_6]]]]$$
$$-[m_2,[m_5,[m_3,[m_4,m_6]]]]+[m_5,[m_2,[m_3,[m_4,m_6]]]].$$

A.2 Proof of Proposition 4.5

To prove that the link in Figure 8 is not relatively slice up to link-homotopy, consider a hypothetical solution shown in Figure 14.

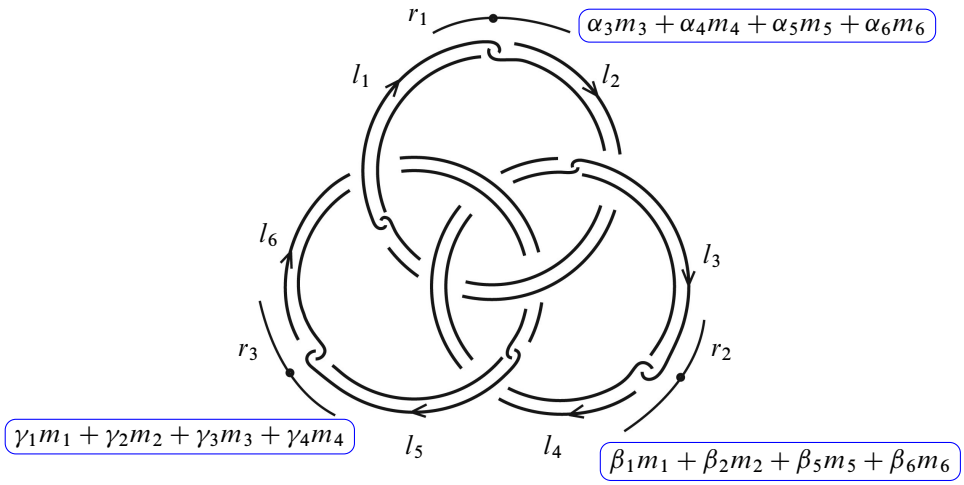

Figure 14: A hypothetical general solution to the relative-slice problem in Figure 8

The circled expressions next to the dotted components show how the slices homologically go over the attached 2–handles (only homological information is relevant, since the calculations below involve 5–fold commutators and all 6–fold commutators are trivial in the Milnor group). Figure 14 shows the general solution: according to Condition 4.1 the slices for l_1, l_2 do not go over the 2–handle attached to r_1, and the analogous restriction

for the other slices. Here the coefficients $\alpha_i, \beta_j, \gamma_k$ are integers, algebraic multiplicities of the hypothetical slices going over the 2–handles. Interpret this as a band-sum of the components $l_1, \dots, l_6$ with parallel copies of r_1, r_2, r_3, yielding a link $(l_1', \dots, l_6')$. A direct analogue of Proposition 3.2 shows that omitting the first component gives a homotopically trivial link, so $M\pi_1(S^3 \smallsetminus (l_2' \cup \cdots \cup l_6')) \cong MF_{m_2,\dots,m_6}$.

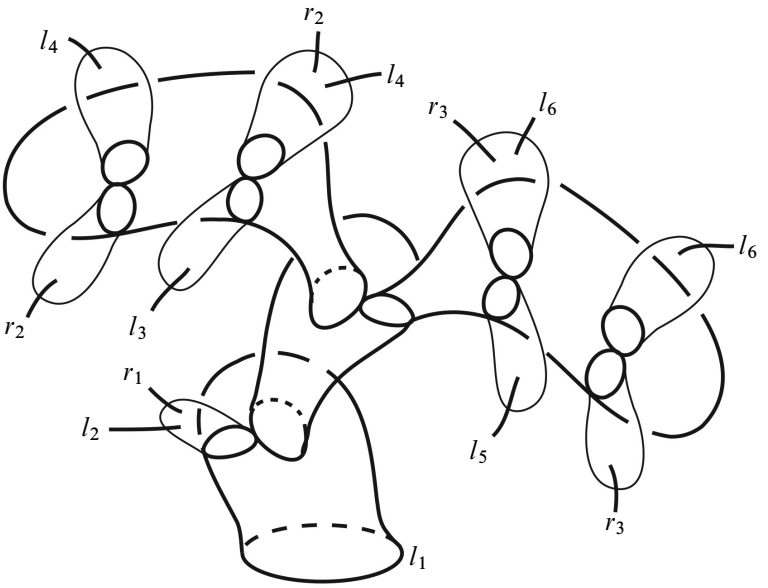

Figure 15: A capped grope bounded by l_1 in Figure 14

The component l_1 bounds a capped grope in S^3, shown in Figure 15. The body (consisting of the surface stages) of the grope is embedded in the complement of the rest of the link in the 3–sphere, and the caps intersect the components $l_2, \dots, l_6, r_1, r_2, r_3$ as indicated in the figure. This grope is a version of the grope shown in the context of the Hopf link in Figures 4 and 5, found in the setting of the Borromean rings. It is not a *half-grope* considered in Section 3.3, but rather a grope of a more general type. Specifically, the two third stage surfaces are attached to a full symplectic basis of the second stage surface, similarly to *symmetric gropes* considered in [4]. (Since the second stage surface has genus one, a symplectic basis consists of two embedded curves forming a basis of the first homology of the surface.) Gropes of the type shown in Figure 15 are a geometric analogue of commutators of the form (4-2).

A geometrically transparent way of identifying the individual commutator summands of l_1' of the form (4-2) is to use the grope splitting technique of the author [5]. Alternatively, this may be done using the commutator identity (3-5), generalizing the argument

in Section 3.3. For the relative-slice problem in Figure 14 to have a link-homotopy solution, l_1' must equal the element w in Lemma 4.3. Collecting the coefficients of each commutator in the definition of w, one gets the following system of equations:

(A-1)	$[m_2,[[m_3,m_4],[m_5,m_6]]]$	$1=1$
(A-2)	$[m_2,[[m_4,m_5],[m_3,m_6]]]$	$\beta_6\gamma_4-\beta_5\gamma_3=1$
(A-3)	$[m_2,[[m_5,m_3],[m_4,m_6]]]$	$\beta_6\gamma_3-\beta_5\gamma_4=1$
(A-4)	$[m_3,[[m_4,m_2],[m_5,m_6]]]$	$-\alpha_3\beta_2+\beta_1\alpha_4=1$
(A-5)	$[m_3,[[m_2,m_5],[m_4,m_6]]]$	$-\alpha_3\beta_6\gamma_2-\beta_1\alpha_5\gamma_4=1$
(A-6)	$[m_3,[[m_5,m_4],[m_2,m_6]]]$	$\alpha_3\beta_5\gamma_2+\beta_1\alpha_6\gamma_4=1$
(A-7)	$[m_4,[[m_2,m_3],[m_5,m_6]]]$	$-\alpha_4\beta_2+\beta_1\alpha_3=1$
(A-8)	$[m_4,[[m_5,m_2],[m_3,m_6]]]$	$-\alpha_4\beta_6\gamma_2-\beta_1\alpha_5\gamma_3=1$
(A-9)	$[m_4,[[m_3,m_5],[m_2,m_6]]]$	$\alpha_4\beta_5\gamma_2+\beta_1\alpha_6\gamma_3=1$
(A-10)	$[m_5,[[m_3,m_2],[m_4,m_6]]]$	$\alpha_5\beta_2\gamma_4-\gamma_1\alpha_3\beta_6=1$
(A-11)	$[m_5,[[m_2,m_4],[m_3,m_6]]]$	$\alpha_5\beta_2\gamma_3-\gamma_1\alpha_4\beta_6=1$
(A-12)	$[m_5,[[m_3,m_4],[m_2,m_6]]]$	$\alpha_5\gamma_2+\gamma_1\alpha_6=1$
(A-13)	$[m_6,[[m_2,m_3],[m_4,m_5]]]$	$\alpha_6\beta_2\gamma_4-\gamma_1\alpha_3\beta_5=1$
(A-14)	$[m_6,[[m_4,m_2],[m_3,m_5]]]$	$\alpha_6\beta_2\gamma_3-\gamma_1\alpha_4\beta_5=1$
(A-15)	$[m_6,[[m_2,m_5],[m_3,m_4]]]$	$\alpha_6\gamma_2+\gamma_1\alpha_5=1$

The first commutator is already present in the expression for l_1 without the relator curves, see (4-1), and there are no further contributions from the relator curves, so (1) is automatically satisfied. There are 14 remaining equations in 12 variables. It is possible to exploit various symmetries of the equations and analyze them by hand, however for the sake of a concise exposition a Mathematica calculation is included below. There are in fact three families of solutions, however there are no *integral* solutions that are relevant for the geometric problem at hand. The "closest" it gets to integers are rational solutions in the first family given in the Mathematica output:

$$\begin{aligned}
&\alpha_3=-1, \quad \alpha_4=-1, \quad \alpha_5=-2, \quad \alpha_6=-2,\\
&\beta_1=1, \quad \beta_2=2, \quad \beta_5=1, \quad \beta_6=-3,\\
&\gamma_1=0, \quad \gamma_2=-\tfrac{1}{2}, \quad \gamma_3=-\tfrac{1}{4}, \quad \gamma_4=-\tfrac{1}{4}.
\end{aligned}$$

A nonintegral solution as above does not seem to have a geometric interpretation in the context of the relative-slice problem.

A.3 Mathematica calculation

This section contains the Mathematica program for solving the system of equations in Appendix A.2, followed by the program output discussed above.

$$
\begin{aligned}
&\text{Solve}[\, b[6]c[4]-b[5]c[3]==1 \;\&\&\\
&\quad b[6]c[3]-b[5]c[4]==1 \;\&\&\\
&\quad -a[3]b[2]+b[1]a[4]==1 \;\&\&\\
&\quad -a[3]b[6]c[2]-b[1]a[5]c[4]==1 \;\&\&\\
&\quad a[3]b[5]c[2]+b[1]a[6]c[4]==1 \;\&\&\\
&\quad -a[4]b[2]+b[1]a[3]==1 \;\&\&\\
&\quad -a[4]b[6]c[2]-b[1]a[5]c[3]==1 \;\&\&\\
&\quad a[4]b[5]c[2]+b[1]a[6]c[3]==1{=}=1 \;\&\&\\
&\quad a[5]b[2]c[4]-c[1]a[3]b[6]==1 \;\&\&\\
&\quad a[5]b[2]c[3]-c[1]a[4]b[6]==1 \;\&\&\\
&\quad a[5]c[2]+c[1]a[6]==1 \;\&\&\\
&\quad a[6]b[2]c[4]-c[1]a[3]b[5]==1 \;\&\&\\
&\quad a[6]b[2]c[3]-c[1]a[4]b[5]==1 \;\&\&\\
&\quad a[6]c[2]+c[1]a[5]==1,\\
&\quad \{a[3],a[4],a[5],a[6],b[1],b[2],b[5],b[6],c[1],c[2],c[3],c[4]\}]
\end{aligned}
$$

Output :

$$
\begin{aligned}
&\Big\{\Big\{a[3]\to -\tfrac{1}{b[1]},\quad a[4]\to -\tfrac{1}{b[1]},\quad a[5]\to -\tfrac{2b[5]}{b[1]},\quad a[6]\to -\tfrac{2b[5]}{b[1]},\quad b[2]\to 2b[1],\\
&\qquad b[6]\to -3b[5],\quad c[1]\to 0,\quad c[2]\to -\tfrac{b[1]}{2b[5]},\quad c[3]\to -\tfrac{1}{4b[5]},\quad c[4]\to -\tfrac{1}{4b[5]}\Big\},\\
&\Big\{a[3]\to -\tfrac{\sqrt{3}}{2b[1]},\quad a[4]\to -\tfrac{\sqrt{3}}{2b[1]},\quad a[5]\to 0,\quad a[6]\to \tfrac{3(-5b[5]-3\sqrt{3}b[5])}{2(3b[1]+2\sqrt{3}b[1])},\\
&\qquad b[2]\to \tfrac{1}{3}(3b[1]+2\sqrt{3}b[1]),\quad b[6]\to -b[5]-\sqrt{3}b[5],\quad c[1]\to -\tfrac{2(3b[1]+2\sqrt{3}b[1])}{3(5+3\sqrt{3})b[5]},\\
&\qquad c[2]\to -\tfrac{2(3b[1]+2\sqrt{3}b[1])}{3(5+3\sqrt{3})b[5]},\quad c[3]\to \tfrac{-1-\sqrt{3}}{(5+3\sqrt{3})b[5]},\quad c[4]\to \tfrac{-1-\sqrt{3}}{(5+3\sqrt{3})b[5]}\Big\},\\
&\Big\{a[3]\to \tfrac{\sqrt{3}}{2b[1]},\quad a[4]\to \tfrac{\sqrt{3}}{2b[1]},\quad a[5]\to 0,\quad a[6]\to \tfrac{3(5b[5]-3\sqrt{3}b[5])}{2(-3b[1]+2\sqrt{3}b[1])},\\
&\qquad b[2]\to \tfrac{1}{3}(3b[1]-2\sqrt{3}b[1]),\quad b[6]\to -b[5]+\sqrt{3}b[5],\quad c[1]\to -\tfrac{2(-3b[1]+2\sqrt{3}b[1])}{3(-5+3\sqrt{3})b[5]},\\
&\qquad c[2]\to -\tfrac{2(-3+2\sqrt{3})b[1]}{3(-5+3\sqrt{3})b[5]},\quad c[3]\to \tfrac{1-\sqrt{3}}{(-5+3\sqrt{3})b[5]},\quad c[4]\to \tfrac{1-\sqrt{3}}{(-5+3\sqrt{3})b[5]}\Big\}\Big\}
\end{aligned}
$$

Acknowledgements I would like to thank Michael Freedman for many discussions on the subject, and Jim Conant for sharing his insight on commutator calculus, in particular an elegant proof of Lemma 4.3. I also would like to thank the referee for helpful comments which improved the exposition of the paper.

I am grateful to the Max Planck Institute for Mathematics in Bonn for hospitality and support. This research was supported in part by NSF grants DMS-1007342 and DMS-1309178.

References

[1] **M H Freedman**, *A geometric reformulation of* 4*–dimensional surgery*, Topology Appl. 24 (1986) 133–141 MR872483

[2] **M H Freedman**, **V Krushkal**, *Topological arbiters*, J. Topol. 5 (2012) 226–247 MR2897055

[3] **M H Freedman**, **X-S Lin**, *On the* (A, B)*–slice problem*, Topology 28 (1989) 91–110 MR991101

[4] **M H Freedman**, **F Quinn**, *Topology of* 4*–manifolds*, Princeton Math. Series 39, Princeton Univ. Press (1990) MR1201584

[5] **V S Krushkal**, *Exponential separation in* 4*–manifolds*, Geom. Topol. 4 (2000) 397–405 MR1796497

[6] **V S Krushkal**, *A counterexample to the strong version of Freedman's conjecture*, Ann. of Math. 168 (2008) 675–693 MR2434888

[7] **V S Krushkal**, *Robust four-manifolds and robust embeddings*, Pacific J. Math. 248 (2010) 191–202 MR2734171

[8] **W Magnus**, **A Karrass**, **D Solitar**, *Combinatorial group theory: Presentations of groups in terms of generators and relations*, Interscience, New York (1966) MR0207802

[9] **J Milnor**, *Link groups*, Ann. of Math. 59 (1954) 177–195 MR0071020

Department of Mathematics, University of Virginia
Charlottesville, VA 22904, USA

krushkal@virginia.edu

http://www.math.virginia.edu/~vk6e

Proposed: Robion Kirby Received: 25 February 2014
Seconded: Michael Freedman, Walter Neumann Revised: 5 August 2014